DOI 10.1007/s10559-015-9762-5
Cybernetics and Systems Analysis, Vol. 51, No. 5, September, 2015

IMAGE SEGMENTATION BASED ON THE EVALUATION OF THE TENDENCY OF IMAGE ELEMENTS TO FORM CLUSTERS WITH THE HELP OF POINT FIELD CHARACTERISTICS

R. J. Kosarevych,[1†] **B. P. Rusyn,**[1‡] **V. V. Korniy,**[1††] **and T. I. Kerod**[1]

UDC 004.932.4

Abstract. *A new approach to the segmentation of an image is proposed on the basis of modeling the spatial distribution of points in the image plane and their ability to identify clusters. Based on detected histogram peaks, a sequence of dominant brightness values (brightnesses) is formed for each fragment of the image. Point fields are formed for each image brightness and the presence of clusters is checked with the help of second-order characteristics of these point fields. The union of all the brightnesses for which point fields form clusters forms the object of segmentation. The results of segmentation of several images are given as compared with those of the thresholding and seed region growing methods.*

Keywords: *image segmentation, clusterization, point field, spatial distribution, local extremum.*

INTRODUCTION

Image segmentation is the first and one of the most important stages in analyzing images. It consists of the classification of pixels of an image into different regions depending on their similarity with respect to definite characteristics. The importance of segmentation is stipulated by the fact that its results directly exert influence on all other stages of image analysis. It is obvious that the formation of characteristics of an object, its classification, and reliable recognition depend to a large extent on the results of segmentation of an image. Moreover, at this stage, images often are strongly distorted. The set of applications of image segmentation varies from the detection of sick cells in a tissue to building identification using remote surface sensing.

The variety of practical applications of segmentation requires the development of various image segmentation methods. Nevertheless, there is still no general image segmentation theory, and, therefore, publications include a wide variety of segmentation algorithms. Different schemes are proposed for the classification of numerous image segmentation methods [1–4]. The majority of well-known methods can be divided into the following two categories: the detection of edges in an image and detection of homogeneous regions.

Methods for detecting homogeneous regions make it possible to single out such regions on the basis of the similarity of their image elements in accordance with a given collection of their characteristics. These regions can be “grown,” united, or divided in the course of segmentation. The thresholding, clusterization, and merging–splitting of regions and graph-based methods all can be considered as methods for detecting regions in an image. From the viewpoint of implementation, the use of cluster analysis methods [5–10] for segmentation is efficient. The essence of clusterization is as follows: all initial objects (pixels in this case) are divided into several disjoint groups so that the objects belonging to one group have similar characteristics whereas the characteristics of objects from different groups must be considerably different. The obtained groups are called clusters. In the simplest method, initial values for clusterization are pixel coordinates. In more complicated cases, for example, for grayscale images, a three-dimensional vector is used that also includes gray gradations in addition to

[1]G. V. Karpenko Physico-Mechanical Institute, National Academy of Sciences of Ukraine, Lviv, Ukraine, [†]*kosarevych@ipm.lviv.ua*; [‡]*rusyn@ipm.lviv.ua*; [††]*valia@ipm.lviv.ua*. Translated from Kibernetika i Sistemnyi Analiz, No. 5, September–October, 2015, pp. 45–55. Original article submitted November 5, 2014.

 1060-0396/15/5105-0704

coordinates. The main problem of clusterization methods is that the spatial arrangement of points either is not taken into account at all or is taken into account only implicitly (for example, using the coordinates of a point as one of features). Therefore, the procedure of selection of connected components is usually executed after clustering points of an image.

The results of clustering noisy images are unsatisfactory since some points are lost and many small regions are formed. At the same time, in the case of large images and the need for partitioning into several classes, cluster analysis methods require intensive computations [9]. A way of decreasing the amount of computations consists of applying them not to all elements of an image but only to a part of them [10]. This can be achieved, for example, by using a method for reducing dimensionality, in particular, the method of principal components, though its use is also connected with large computational complexity.

The present article proposes an approach to image segmentation on the basis of evaluating (with the help of point fields) the tendency of a set of points to form clusters.

DESCRIPTION OF POINT FIELDS

Random point fields (or spatial point processes) are natural models for spatial data that represent configurations of points. These data are often called point sets or point patterns. Random point fields often occur in a variety of scientific disciplines including seismology, ecology, forestry, epidemiology, economics, materials science, etc. [11–16]. But common to all of them is that, first, random events occur in physical space and, second, these events are not independent.

It is supposed that point configurations $x = \{x_1, x_2, \dots, x_i, \dots\}$, where $x_i \in S$ is a complete separable space, are locally finite. A configuration is understood to be a set of unordered points. If the space S itself is bounded or the number of all points in any configuration is finite, i.e., $n(x_S) < \infty$, then the point field is called finite. Next, we assume that $S = D$, where $D \subset R^d$.

A homogeneous Poisson point field is a fundamental model in stochastic geometry. In the majority of cases, on the basis of this model, theoretical results can be obtained. Moreover, it plays the role of a reference model with respect to which many other models are considered. A Poisson point field formalizes the ideas about "perfect" randomness, which is expressed in the absence of a definite structure of a set of points representing a realization of a point field. Therefore, the majority of investigations of point fields begin with testing the hypothesis of complete spatial randomness (CSR) of such a field, i.e., its correspondence with a Poisson point field [17]. The lack of correspondence allows one to assume that he deals with a nonrandom point pattern is, i.e., to consider that points are regularly arranged or that there are aggregations (clusters) of points [18] (Fig. 1).

One of methods for detecting the presence of clusters in a point configuration is the analysis of the distribution function of the distance to its closest neighbor in the point field. In the presence of clusters, this function assumes larger values than for Poisson fields with the same number of points per unit area. However, the so-called K-function proposed by B. Ripley [19] is more often used. The K-function, namely, $K(r)$, where r is the distance equal to the radius of the neighborhood of elements that is analyzed in the point field, it is found as the averaged number of elements of the point field that are different from the chosen one and is normalized by the intensity of elements of the point field. The simplest estimate for the K-function is of the form

$$\hat{K}(r) = \hat{\lambda}^{-1} \frac{1}{N} \sum_{i=1}^{N} \sum_{j=1,\, j \neq i}^{N} \delta(d(x_i, x_j) < r),$$

where N is the number of field elements; $\hat{\lambda}$ is an intensity estimate; $d(x_i, x_j)$ is the distance between points x_i and x_j; $\delta(d(x_i, x_j) < r) = 1$ if $d(x_i, x_j) < r$ and $\delta(d(x_i, x_j) < r) = 0$ otherwise. To obtain a more reliable estimate for the K-function, a more exact estimate for the intensity λ is used in the form $\hat{\lambda}^2 = N(N-1)/A^2$, where A is the area of the region S, and also the influence of the marginal field elements is taken into account when a circle part is outside of the region S. Then the expression for estimating the K-function is of the form [20, 21]

$$\hat{K}(r) = \frac{1}{\hat{\lambda}^2 A} \sum_{i=1}^{N} \sum_{j=1,\, j \neq i}^{N} (w_{ij}^{-1}) \delta(d(x_i, x_j) < r),$$

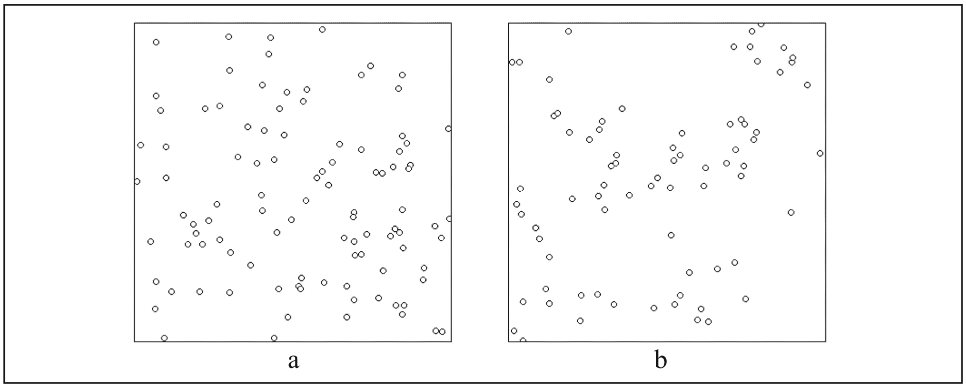

Fig. 1. Random (a) and regular (b) arrangements of elements of a point field.

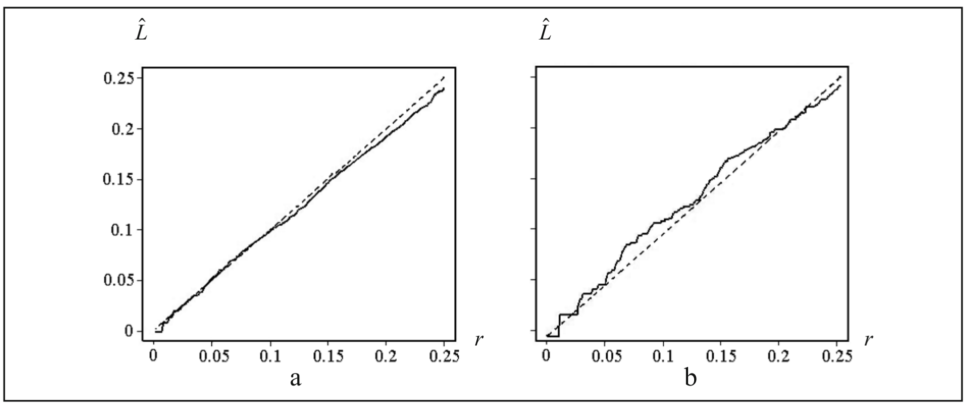

Fig. 2. Dependencies of $\hat{L}(r)$ for random (a) and regular (b) arrangements of elements in a point field (the continuous line) as compared with values of $\hat{L}(r)$ for CSR (the dashed line).

where the averaged number of elements of the point field is normalized by the length of a circle w_{ij} whose center is at the point x_i, that passes through x_j, and that is located within the region S. When intensity is constant, the circle signifies the conditional probability of the existence of a field element x_j located at a distance $d(x_i, x_j)$ from a field element x_i within the region S. Note that $w_{ij} = 1$ when the distance between the points x_i and x_j is less than the distance from x_i to the edge of S.

For a cluster point field, the distances between the majority of points are smaller than those expected under the CSR condition and, therefore, their characteristics have larger values than for a Poisson field with the same distances. In particular, under the CSR condition, $K(r) = \pi r^2$, and, for a cluster point field, $K(r) > \pi r^2$. To increase the illustrativeness of graphical representation of the K-function, the following transformation was proposed [22]:

$$\hat{L}(r) - r = \left(\frac{\hat{K}(r)}{\pi}\right)^{1/2} - r$$

in which the right side is equal to r under the CSR condition and, hence, the subtraction of r assigns the value of the characteristic equal to zero. Constructing the plot of r with respect to $\hat{L}(r)$, one can easily find both the distances for which cluster formations of points exist (Fig. 2a),

$$\hat{L}(r) > r, \tag{1}$$

and the distances for which points are too uniformly arranged to meet the CSR condition $\hat{L}(r) < r$ (Fig. 2b).

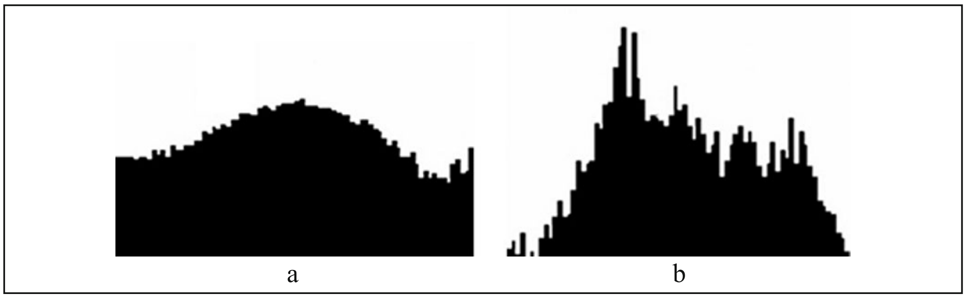

Fig. 3. Histograms of an image with small (a) and large (b) average differences between adjacent values.

FORMATION OF POINT FIELDS FROM IMAGES

Image fragmentation. In analyzing an image, image fragments with forcibly expressed peculiarities of color, form, or position of an object primarily draw attention [23]. Based on brightness values, an object can be easily detected in an image even if it is represented by some set of brightness values. To segment an object, it suffices to choose only the brightnesses that represent it in the image. This is easily attainable, for example, by applying threshold segmentation if the set of brightness values of the object is known but, otherwise, difficulties arise [24].

If a trivial image is considered in which, against a homogeneous background, an object is located whose brightness is also homogeneous, then the histogram of this image is double-mode and its modes correspond to object and background brightnesses. In the case of images with a large range of brightnesses and small objects, the mode corresponding to the object is not necessarily represented in the histogram. If an image is partitioned into fragments commensurate with an object, then the histogram of this fragment contains modes in the range of brightnesses inherent in the object. The presence of modes corresponding to objects of interest considerably simplifies image segmentation. To detect modes in a histogram, algorithms for finding local maxima are used.

Detection of histogram modes. There are many algorithms for finding local maxima. As a rule, they all require the specification of additional parameters [25–28]. Some of them can be found proceeding from input data [27]. The first step of such algorithms usually is the test of each element of the input sequence for a local extremum. This step generates a redundant number of extrema, and some additional conditions are proposed to decrease it. These conditions usually are heuristic. To reduce the number of such conditions, we suggest choosing the neighborhood size for testing local extremum conditions depending on the degree of smoothness of the histogram envelope [5]. When the envelope is a smooth curve as is shown in Fig. 3a, the difference between adjacent histogram values is insignificant. In this case, there is no need to test the local extremum condition in a minimal neighborhood, and a larger neighborhood can be chosen. And vice versa, if an image histogram consists of a large number of extrema that alternate inconsistently as is shown in Fig. 3b, then the difference between adjacent values is larger and the size of the neighborhood being analyzed should be decreased to avoid the loss of an extremum.

Let $H(I)$ be the histogram of an image I. We define the neighborhood size O for finding a local extremum as follows:

$$O = \frac{(M-1)\sum_{i=1}^{M} H(i)}{M \sum_{i=1}^{M-1} |H(i+1) - H(i)|}, \tag{2}$$

where $H(i)$ is the histogram value for a brightness i and M is the number of nonzero values of the histogram. Expression (2) represents the ratio of the average histogram value to the average value of the difference between adjacent values. A larger value of the denominator corresponds to the case when the image histogram includes a set of local extrema that are not sequentially located and lead to a decrease in the size of the neighborhood being analyzed. In the case of a small discrepancy between adjacent histogram values, the value of the denominator decreases, which leads to the increase in the size of the neighborhood O.

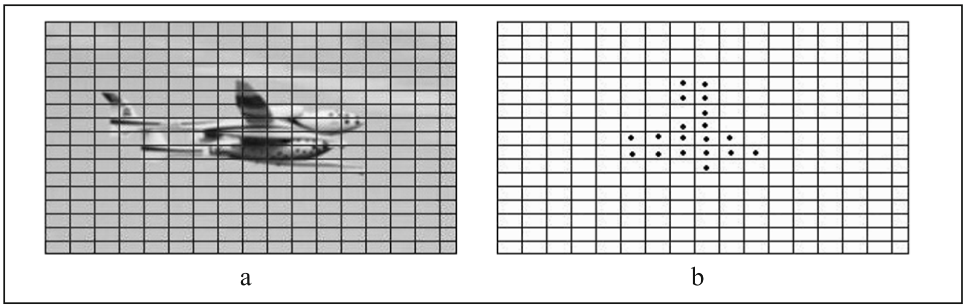

Fig. 4. Formation of a point field on the basis of the brightness value of the initial image (a) and a point field on the basis of the brightness value equal to 207 (b).

Formation of a point field with a certain brightness. An image is divided both horizontally and vertically into equal numbers of fragments (it is not an essential condition). We act on the premise that the choice of an image format is based on conditions of its formation, i.e., the extent of an object is better represented on an image with different dimensions. A significant amount of parts of the object of interest out of the total amount of fragments must enter into one or several fragments (Fig. 4a). In this case, brightnesses in the histogram of a fragment that represent the object form a clear peak or an extremum. We will associate with each fragment the set of extrema of its histogram. For images with the well-separable structure object–background, the assumption is obvious that the points whose brightnesses are constituents of the object form a compact subset. Therefore, selecting the brightnesses with this characteristic in the image, the object of interest can be singled out.

Let us form a point field for each brightness value from the range of image brightness values. The size of such a point field corresponds to the size of the image that is divided into the same number of fragments. We will mark the center of a fragment if the value of the brightness being considered belongs to the associated set of the fragment of the initial image. Thus, we obtain the set of points whose arrangement shows the prevalence of the brightness being considered in the image (Fig. 4b).

Next, the hypothesis of the complete spatial randomness of the field should be confirmed or refuted. In order to make sure that the field being considered contains clusters of points, the fulfillment of condition (1) should be checked. To this end, it is natural to use the *L*-test defined as follows:

$$\tau = \max_{r \le s} | \hat{L}(r) - r | ,$$

where s is the upper bound on the length of distances between field points [21]. If the value of τ is too large, then the hypothesis of the complete spatial randomness of the field should be ruled out. The critical value of τ for the significance value $\alpha = 0.05$ is determined from the expression $\tau_{0.05} = 1.45\sqrt{a} / n$, where a is the number of fragments into which the image is divided and n is the number of elements of the point field. The quantity s corresponds to half of the diagonal of the region in which the point field is located [19].

If the formation of clusters is inherent in elements of a point field, then we fix the value of the brightness for which it has been formed. After an exhaustive search of all image brightnesses, some set $B = [int_1, int_2, \dots, int_k]$ is formed that contains the brightnesses forming aggregations of points in the image. The selection of exactly these image brightnesses allows one to segment the object of interest.

SEGMENTATION RESULTS AND A DISCUSSION

Figure 5 presents the results of segmentation of an image with the help of well-known approaches such as the Canny edge-detection [29], Otsu thresholding method [30], seed region growing method [31], and the proposed method. The results obtained with the help of the seed region growing method (Fig. 5c) and the method proposed (Fig. 5d) in the present article are more preferable than the results obtained by the Canny [29] and Otsu [30] methods. This is explained by the fact that the first two approaches as opposed to the two latter use information on the interrelation between image elements. Image

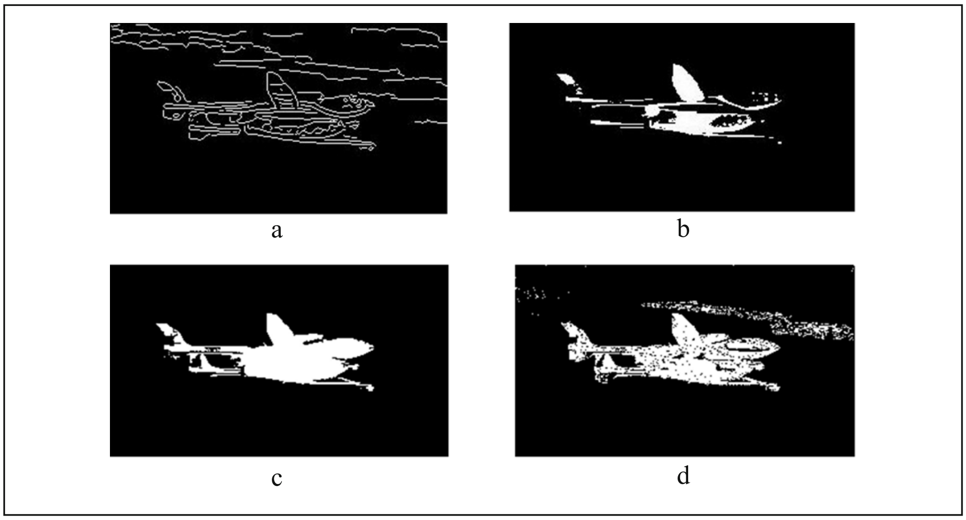

Fig. 5. Image segmentation with the help of the Canny method (a), Otsu method (b), seed region growing method (c), and proposed method (d).

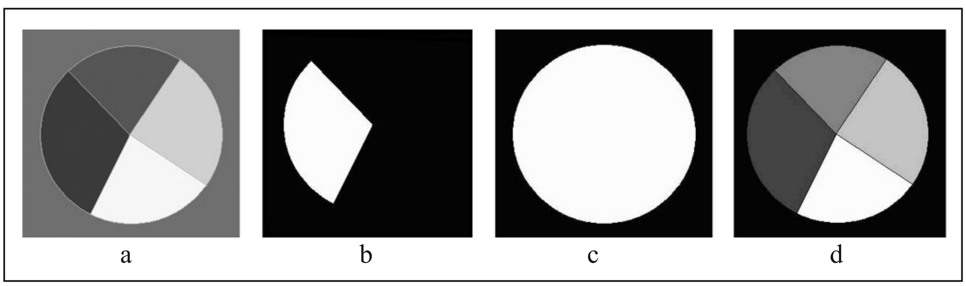

Fig. 6. Segmentation of the initial image (a) by the seed region growing method with different initial regions (b and c), and by the proposed method (d).

segmentation with the help of edge-detection yields satisfactory results in the case of the uniform brightness distribution over the image and a distinguished boundary between the object and background. In the other cases, as a result of this segmentation, some discontinuities along the edge line or false contours occur. As a rule, an additional image post-processing is required (Fig. 5a). Threshold segmentation also makes it possible to single out the entire object only in the case of uniform image brightness distribution but, otherwise, parts of the object may be lost (Fig. 5b). As is well known, the seed region growing methods are initialized by initial regions or points in the image and, based on homogeneity criteria, partition the image into connected components each of which contains an initial region. This implies the main drawback of such methods, namely, the dependence of the obtained results on arrangements of initial regions in the image. In other words, considerably different segmentation results can be obtained. The image presented in Fig. 6a demonstrates the influence of a change in the positions of initial regions on the obtained result even in this simple case (Figs. 6b and 6c). A special question is connected with the number of initial regions required for image segmentation.

The proposed method is generally devoid of the mentioned drawbacks. In the case when the object of interest is represented in the image by a set of brightnesses, the selection of a relevant fragment size makes it possible to form the corresponding peak on the histogram and to add the corresponding brightness to the set B. For the image segmentation problem, cases are not infrequent when there is no need to single out the entire object, and only its fragments are considered. In this case, elements of the set B are not united.

Figure 6d presents the result of segmentation of fragments of the object presented in Fig. 6a.

To compare the results of different segmentation algorithms, standardized sets of images are used [32]. The results of application of the proposed method and comparison of its results with those of other segmentation methods are presented in Fig. 7. To quantitatively estimate the results, the quantities proposed in [33, 34] are used. One of the obtained estimates,

TABLE 1

Image Number According to Fig. 7	***ME* Estimate for the Following Methods:**		
	Otsu method	seed region growing method	proposed method
1	0.01290	0.02280	0.08176
2	0.01259	0.06375	0.08939
3	0.07404	0.13467	0.24695
4	0.97774	0.35962	0.21003
5	0.18564	0.11902	0.07227

TABLE 2

Image Number According to Fig. 7	***RAE* Estimate for the Following Methods:**		
	Otsu method	seed region growing method	proposed method
1	0.95892	0.01639	0.04648
2	0.01467	0.06728	0.03675
3	0.09949	0.16638	0.20101
4	0.61557	0.50921	0.14311
5	0.22932	0.12818	0.06033

namely, the incorrect classification error *ME* [33] reflects the ratio between the points of the background of an image that are ascribed to an object and, vice versa, the points of the object classified as background points. For the problem of two-level segmentation of the image being tested, the estimate *ME* is expressed as follows:

$$ME = 1 - \frac{|B_O \cap B_T| + |F_O \cap F_T|}{|B_O| + |F_O|},$$

where B_O and F_O denote the sets of points that belong to the object and to the background of the image and are obtained as a result of an objective expert segmentation B_T and F_T are the same sets obtained as a result of application of a segmentation method to the test image. The *ME* value varies from zero in the case of an ideal segmentation to one in the case of a completely incorrect segmentation. Another estimate for an incorrect classification, namely, *RAE* [34] uses the comparison of the areas of the object singled out as a result of expert segmentation and that singled out with the help of a method and is expressed as follows:

$$RAE = \begin{cases} \dfrac{A_O - A_T}{A_O} & \text{if } A_T < A_O, \\ \dfrac{A_T - A_O}{A_T} & \text{if } A_T \ge A_O, \end{cases}$$

where A_O is the area obtained as a result of expert segmentation and A_T is the area obtained by a segmentation method. As well as in the case of the incorrect classification error *ME*, the value of *RAE* varies in the range $[0, 1]$ depending on segmentation quality. The results of computation of the estimates *ME* and *RAE* are presented in Tables 1 and 2, respectively. The numbers in the first column of both tables are serial numbers of the images presented in Fig. 7.

The comparison of the results of segmentation and values of quantitative estimates shows that the subjective perception of the results does not necessarily coincide with their estimates expressed in quantitative terms. In particular, for the first image in the 3th row in Fig. 7, better values of the estimates *ME* and *RAE* are obtained for the seed region growing method and Otsu method than for the proposed method, though a more exact correspondence between the initial image and the result of segmentation by the proposed method can be visually verified. This implies that, even for the simplest case of classification of an image into two classes, quality estimates based on simple characteristics such as area or perimeter are not always correct. In this case, the estimates *ME* and *RAE* are formed on the basis of their comparison with expert segmentation obtained by manual threshold selection (binarization).

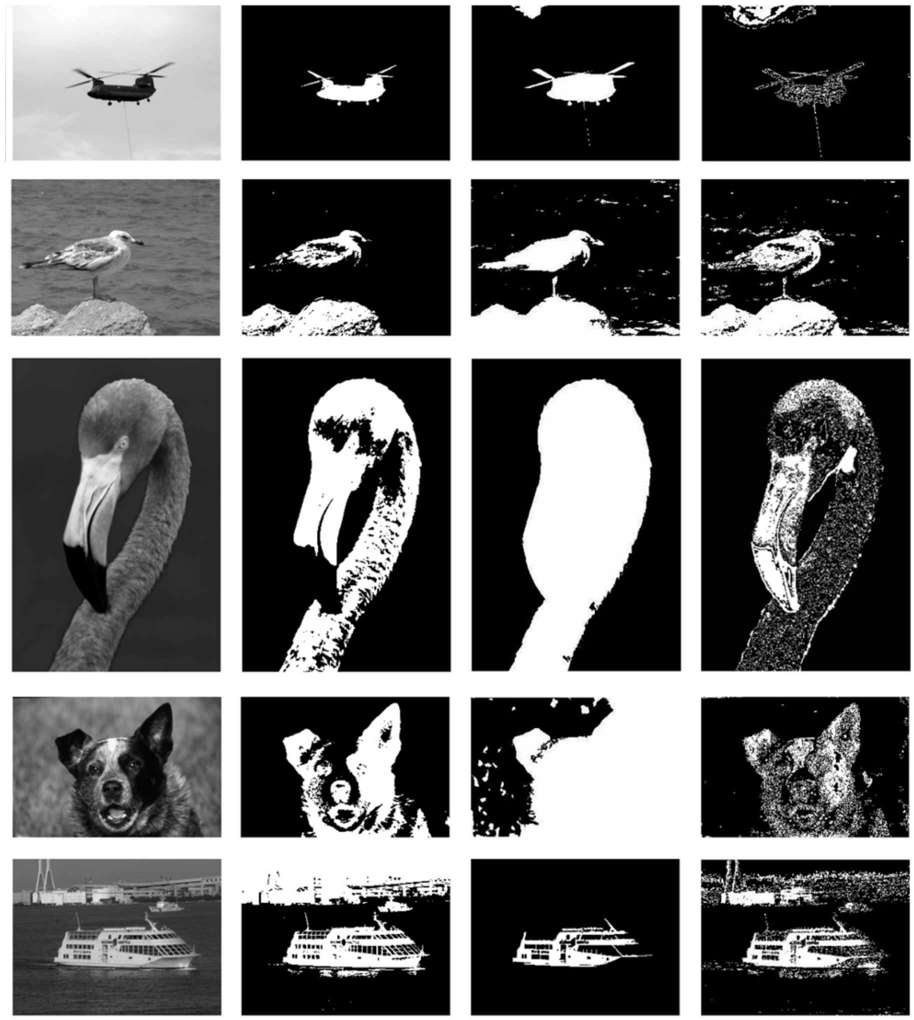

a b c d

Fig. 7. Segmentation of the initial images (a) by the Otsu method (b), seed region growing method (c), and proposed method (d).

It should be noted that the results of segmentation by the proposed method can require post-processing since an object (even a simple one) is hardly ever represented in a real image by a single brightness value. However, the application of the proposed segmentation method makes it possible to more properly single out peculiarities of the object form that, in turn, is an important feature for recognition systems [4].

CONCLUSIONS

A new approach to image segmentation is proposed that is based on the assumption that the set of brightnesses representing an object form sets of points tending to the formation of clusters. For detecting such brightnesses, we form point fields and, among them, choose the fields for which the L-test conditions are satisfied. The application of this approach to image segmentation is stipulated by the fact that cluster rather than regular or random aggregations are more widespread in the real world.

Various models are proposed for detecting such aggregations. At present, a homogeneous Poisson process is used as the basis for the development of models for describing point fields and testing their CSR. If data conform to such a model, then more complicated models are not considered.

The investigations performed show that, for a more exact segmentation of images, complicated models of point fields should be used. The simplest way consists of introducing the intensity function of a Poisson process. In this case, a constant intensity of the process is replaced with a function whose value varies depending on a position. A widespread approach to the modeling of aggregations of points is the use of "nested" Poisson processes such as Cox, Matérn, and Neyman–Scott processes. These processes consist of a "parent" Poisson process and "affiliated" Poisson processes formed around the elements of the "parent" process. A large class of Markov point fields allows one to take into account the interaction between elements when the change in the value of the potential function for field elements from positive to negative changes a regular pattern of their arrangement to a cluster arrangement.

REFERENCES

1. K. S. Fu and J. K. Mui, "A survey on image segmentation," Pattern Recognition, **13**, No. 1, 3–16 (1981).
2. N. R. Pal and S. K. Pal, "A review on image segmentation techniques," Pattern Recognition, **26**, No. 9, 1277–1294 (1993).
3. Y. J. Zhang, Advances in Image and Video Segmentation, IRM Press, London (2006).
4. S. Belongie, J. Malik, and J. Puzicha, "A survey on image segmentation," IEEE Transaction on Pattern Analysis and Machine Intelligence, **24**, No. 4, 509–522 (2002).
5. R. J. Kosarevych, M. I. Kobasyar, and B. P. Rusyn, "Multilevel thresholding by clustering the set of extrema of histograms of image fragments," Information Extraction and Processing, Issue 34 (110), 113–119 (2011).
6. A. Jain, M. Murty, and P. Flynn, "Data clustering: A review," ACM Computing Surveys, **31**, No. 3, 264–323 (1999).
7. S. P. Lloyd, "Least squares quantization in PCM," IEEE Transaction on Information Theory, **28**, No. 2, 129–137 (1982).
8. P. Yang and S. Huang, "Image segmentation by fuzzy c-means clustering algorithm with a novel penalty term," Computing and Informatics, **26**, No. 1, 17–31 (2007).
9. S. Thilagamani and N. Shanthi, "A survey on image segmentation through clustering," International Journal of Research and Reviews in Information Sciences, **1**, No. 1, 129–137 (2011).
10. L. A. Waller, "Detection clustering in spatial data," in: A. S. Fotheringham and P. A. Rogerson (eds.), The Sage Handbook of Spatial Analysis, Sage Publications Inc., Thousand Oaks, CA (2009), pp. 299–320.
11. J. M. Albert, M. R. Casanova, and V. Orts, "Spatial location patterns of Spanish manufacturing firms," Papers in Regional Science, **91**, No. 1, 107–136 (2012).
12. I. Alcobia, A. S. Quina, H. Neves, N. Clode, and L. Parreira, "The spatial organization of centromeric heterochromatin during normal human lymphopoiesis," Experimental Cell Research, **290**, No. 2, 358–369 (2003).
13. P. Haase, "Spatial pattern analysis in ecology based on Ripley's K-function: Introduction and methods of edge correction," Journal of Vegetation Science, **6**, No. 4, 575–582 (1995).
14. N. Raghavan and P. K. Goel, "Modeling and characterizing microstructures using spatial point processes," Statistical Computing & Statistical Graphics Newsletter, **8**, No. 2/3, 10–16 (1997).
15. D. Stoyan and A. Penttinen, "Recent applications of point process methods in forestry statistics," Statistical Science, **15**, No. 1, 61–78 (2000).
16. K. Vasudevan, S. Eckel, F. Fleischer, V. Schmidt, and F. Cook, "Statistical analysis of spatial point patterns on deep seismic region data: A preliminary test," Geophysical Journal International, **171**, No. 2, 823–840 (2007).
17. B. Ripley, "Test of randomness for spatial point patterns," Journal of the Royal Statistical Society, **41**, No. 3, 368–374 (1979).
18. D. J. Gates and M. Westcott, "Clustering estimates for spatial point distributions with unstable potentials," Annals of the Institute of Statistical Mathematics, **38**, No. 1, 123–135 (1986).
19. B. Ripley, "The second–order analysis of stationary point processes," Journal of Applied Probability, **13**, No. 2, 255–266 (1976).
20. D. Stoyan and H. Stoyan, "Improving ratio estimators of second order point process characteristics," Scandinavian Journal of Statistics, **27**, No. 4, 641–656 (2000).
21. D. Stoyan and H. Stoyan, Fractals, Random Shapes, and Point Fields, Wiley, Chichester (1994).

22. J. Besag, "Discussion of 'Modeling spatial patterns' by B. D. Ripley," Journal of the Royal Statistical Society, **39**, No. 4, 192–225 (1977).
23. V. P. Boyun, "Intelligent selective perception of visual information: Informational aspects," Artificial Intelligence, No. 3, 16–24 (2011).
24. S. Alpert, M. Galun, R. Basri, and A. Brandt, "Image segmentation by probabilistic bottom-up aggregation and cue integration," in: IEEE Conference on Computer Vision and Pattern Recognition (CVPR' 07) (2007), pp. 1–8.
25. L. Xu, "Robust peak detection of pulse waveform using height ratio," in: Proc. 30th Annual Intern. Conf. of the IEEE Engineering in Medical and Biology Society, Vancouver, British Columbia, Canada (2008), pp. 3859–3865.
26. A. Nakib, H. Oulhadj, and P. Siarry, "Image histogram thresholding based on multiobjective optimization," Signal Processing, **87**, No. 11, 2516–2534 (2007).
27. A. L. Jacobson, "Auto-threshold peak detection in physiological signals," in: Proc. 23th Annual Intern. Conf. of the IEEE Engineering in Medical and Biology Society, Istanbul, Turkey (2001), pp. 2194–2195.
28. M. Sezan, "A peak detection algorithm and its application to histogram–based image data reduction," Computer Vision Graphics Image Processing, **49**, No. 1, 36–51 (1990).
29. J. Canny, "A computational approach to edge-detection," IEEE Transaction on Pattern Analysis and Machine Intelligence, **8**, No. 6, 679–698 (1986).
30. N. Otsu, "A threshold selection using grey level histograms," IEEE Transaction on System, Man, and Cybernetics, **9**, No. 1, 62–69 (1979).
31. R. Adams and L. Bischof, "Seed region growing," IEEE Transaction on Pattern Analysis and Machine Intelligence, **16**, No. 6, 641–647 (1994).
32. Segmentation Evaluation Database, http://www.wisdom.weizmann.ac.il/~vision/Seg_Evaluation_DB/index.html.
33. W. Yasnoff, J. K. Mui, and J. W. Bacus, "Error measures for scene segmentation," Pattern Recognition, **9**, No. 4, 217–231 (1977).
34. M. Sezgin and B. Sankur, "Survey over image thresholding techniques and quantitative performance evaluation," Journal of Electronic Imaging, **13**, No. 1, 146–165 (2004).